On the influence of deformation rate on intergranular crack propagation in Type 304 stainless steel

H. NAHM, D. J. MICHEL, J. MOTEFF
Department of Materials Science, and Metallurgical Engineering, University of Cincinnati, Cincinnati, Ohio, USA

The influence of deformation rate on the stable intergranular crack propagation behaviour of Type 304 stainless steel, as reflected in the crack width, length, and angular orientation parameters was examined. Specimens deformed to failure in the slow tension and creep-rupture modes at 650°C were studied. The results indicate that a rapid, step-wise crack propagation between grain-boundary triple junctions does not occur for these specimens, but that the triple junctions do provide a significant barrier to crack propagation. The crack angular orientation and width, as a function of deformation rate, were concluded to be the parameters which reflect the crack growth rate for the test conditions employed in this work.

1. Introduction

The formation of intergranular wedge-type microcracks during slow deformation of austenitic stainless steels at elevated temperatures has been established by previous investigations [1-5]. The experimental results indicate that cracking is often initiated or arrested at grain-boundary triple junctions [1,4,6,7]. Various models have been proposed to explain the wedge-type crack formation and propagation [8-13]. The nature of the intergranular cracking process itself also suggests that crack width and length and crack angular orientation with respect to the applied stress direction are important parameters in understanding the stable crack-propagation behaviour. The purpose of this communication is to examine these parameters with respect to deformation rate for the case of AISI Type 304 stainless steel tested in the slow tension and creep-rupture modes at 650°C.

2. Experimental details

The 304 stainless steel used had the following composition (wt %):

C	Cr	Ni	Mo	Mn	Si	P	S
0.048	18.6	9.7	0.32	1.22	0.48	0.028	0.015

Cylindrical test specimens with 6.35 mm gauge diameters and 50.8 mm gauge lengths were machined from 25.4 mm thick plate with their test axes parallel to the plate rolling direction. The specimens were annealed at 1093°C for 0.5 h and water quenched to give a linear intercept grain size of 210 ± 5 μm. Three tensile and three creep-rupture specimens were tested to failure in air at 650°C. The tensile tests were conducted at steady-state strain-rates of 8.33×10^{-4}sec^{-1}, 8.33×10^{-5}sec^{-1}, and 8.33×10^{-6}sec^{-1}. The creep-rupture tests were conducted at stress levels to produce minimum creep rates of 1.28×10^{-6}sec^{-1}, 2.42×10^{-7} sec^{-1}, and 4.16×10^{-8}sec^{-1}. The test results for these specimens are given in Table I.

Half of each fractured specimen was cut parallel to the stress axis and sectioned to yield metallographic specimens. Each metallographic specimen was ground on silicon carbide paper and given a final polish with 0.05 μm alumina. Examination of the as-polished sections revealed no accumulation of polishing debris in the microcracks. A light etch with a $3HCl:1HNO_3:4H_2O$ solution was sufficient to reveal the grain boundaries. No significant alteration of the crack shape could be detected due to etching. All cracks were sharp (wedge-shaped) and were considered to be those formed during testing. A magnification of 200 times was used to study the cracks over the entire surface of each metallographic specimen.

For the deformation rates employed in the testing, it was frequently observed that the

TABLE I Tensile and creep-rupture test results for 304 stainless steel at 650°C

Tensile results Specimen no.	Strain-rate (sec^{-1})	Ult. tensile stress (kg/mm^2)	Elongation (%)	Reduction in area (%)
1	8.33×10^{-4}	29.5	43.5	29.0
2	8.33×10^{-5}	26.0	34.0	26.0
3	8.33×10^{-6}	21.5	27.5	24.5

Creep-rupture results Specimen no.	Minimum creep-rate (sec^{-1})	Stress (kg/mm^2)	Total elongation (%)	Rupture life (h)
1	1.28×10^{-6}	17.5	25	28
2	2.42×10^{-7}	14.0	25	111
3	4.16×10^{-8}	10.5	21	730

cracks terminated at locations between triple junctions at points not associated with precipitates or twin-boundary intersections, in addition to termination at triple junctions. Therefore, the length of each crack was determined in terms of the fractional number of grain-boundary facets occupied, where applicable. The angular orientation with respect to the applied stress direction was determined for each of these cracks. The crack width (or wedge height) was also determined for the creep-rupture specimens.

3. Results

The crack distributions for those cracks which occupy two grain-boundary facets or less are shown in Fig. 1 as functions of the fractional crack length. The results for cracks which occupy

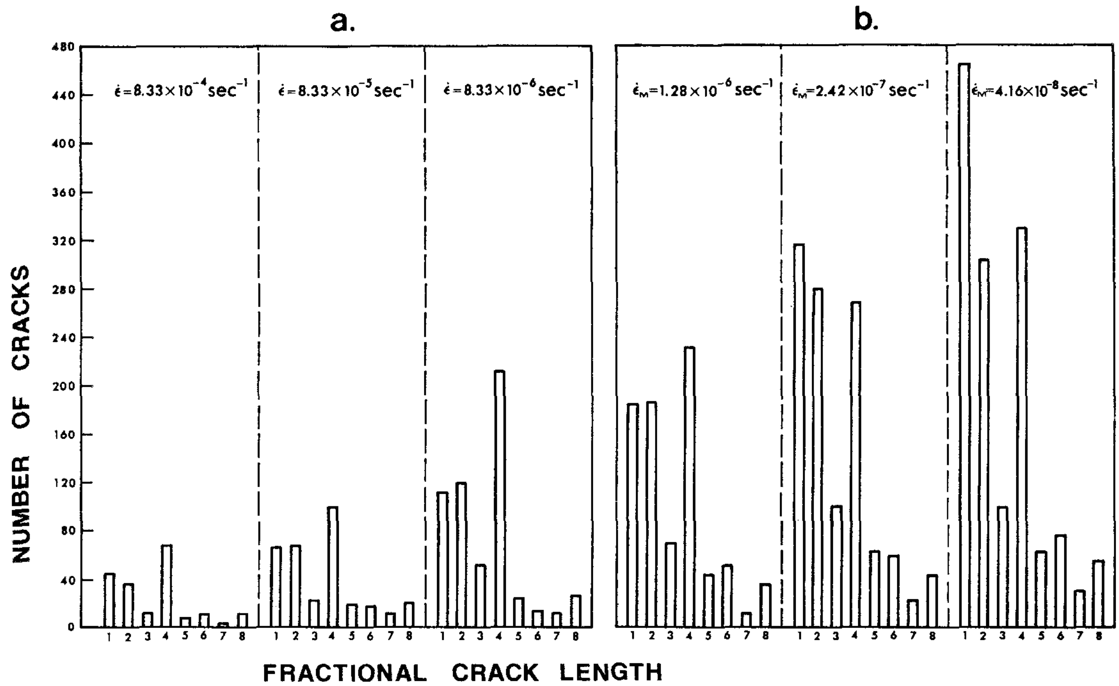

Figure 1 Crack number distribution as a function of fractional crack length for the (a) tensile and (b) creep-rupture specimens. The fractional crack length intervals are: (1) $0 < l \leqq \frac{1}{3}$; (2) $\frac{1}{3} < l \leqq \frac{2}{3}$; (3) $\frac{2}{3} < l < 1$; (4) $l = 1$; (5) $1 < l \leqq 1\frac{1}{3}$; (6) $1\frac{1}{3} < l \leqq 1\frac{2}{3}$; (7) $1\frac{2}{3} < l < 2$; (8) $l = 2$. $\dot{\epsilon}$ = tensile strain rate; $\dot{\epsilon}_m$ = minimum creep rate.

either one or two entire boundary facets have been plotted separately in this figure*. Cracks whose length, l, in terms of grain-boundary facets, is in the range $l \leqq 1$ were found to comprise the majority of cracks ($\sim$ 70%) for each specimen. In addition to those cracks whose lengths fall in the interval $1 < l \leqq 2$, the remaining cracks were either those greater than two facets in length ($\sim$ 7%), assumed to have undergone rapid propagation related to specimen failure, or those associated with annealing twin inter sections($\sim$ 10%). The formation of cavities and cracks on the transgranular twin boundaries has also been observed in these specimens [14].

The largest number of cracks for the tensile specimens occurs where $l = 1$ (Fig. 1a). The creep-rupture specimens show a similar behaviour except that many more small cracks ($0 < l \leqq 2/3$) have formed (Fig. 1b). The number of cracks in each length interval generally increases with decreasing deformation rate.

The measured angular distributions of the cracks are shown in Fig. 2. Separate plots are given for each of the tensile and creep-rupture specimens for cracks whose lengths fall in the intervals $0 < l \leqq \frac{1}{3}$, $\frac{1}{3} < l \leqq \frac{2}{3}$, $\frac{2}{3} < l < 1$ and $l = 1$. No correction to obtain a "true" distribution has been applied to this figure since it has been shown that a measured (or apparent) distribution closely approximates the true distribution [15]. For the tensile specimens, the angular orientation of the maximum crack fraction shifts from $\sim$ 45° to $\sim$ 80° with decreasing strain rate within each fractional crack length interval. However, the angle at which this maximum fraction occurs for a particular tensile specimen remains relatively constant regardless of crack length. The angular orientation of the maximum fraction for the creep-rupture specimens remains essentially constant at $\sim$ 80° irrespective of changes in both crack length and minimum creep rate.

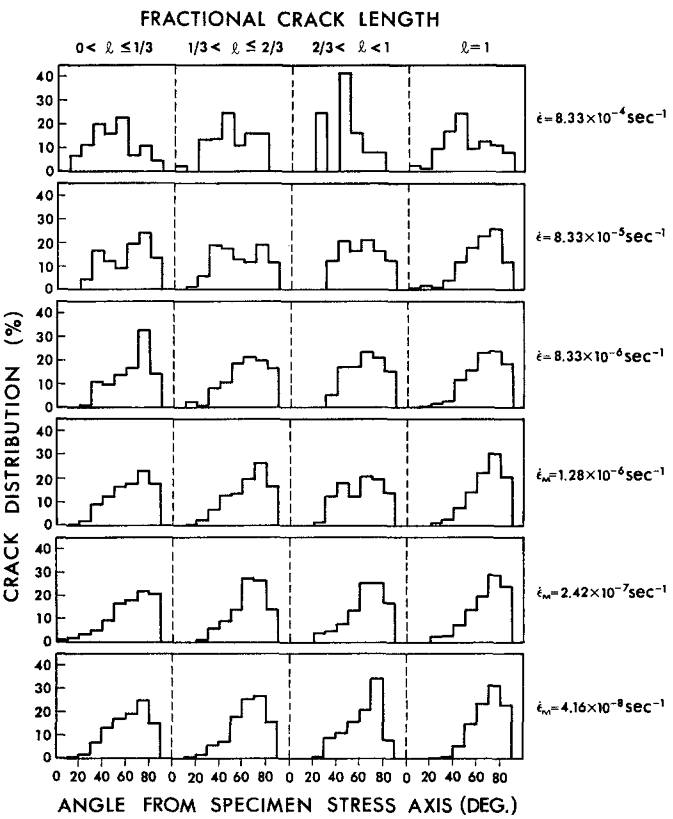

Figure 2 Angular percentage distributions for the tensile and creep-rupture specimens.

*Intervals of thirds were found to be convenient for plotting the fractional facet crack length results

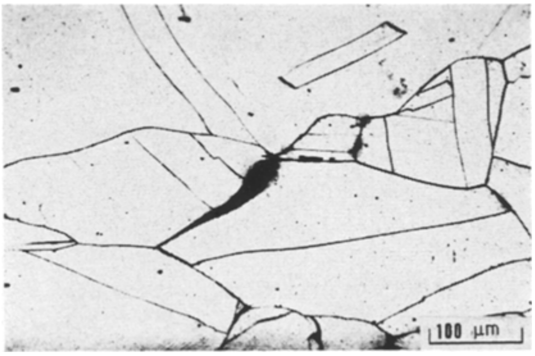

Figure 3 Optical micrograph of a typical wedge-type crack observed in the tensile and creep-rupture specimens. Tensile strain-rate $8.33 \times 10^{-6} sec^{-1}$. Stress axis is horizontal.

A typical example of the wedge-type cracks observed in these specimens is shown in Fig. 3.

4. Discussion

It has been previously observed that virtually all of the wedge-type cracks were arrested at triple junctions for a 20% Cr-35% Ni austenitic stainless steel tested in slow tension at 700° C [1-3]. These observations led to the conclusion that crack growth for this material proceeds in a step-wise manner, with each step constituting a single boundary facet [1,16]. This conclusion has been questioned by Gifkins [17], who suggested that the stable crack length may be of the order of 1.5 facets, instead of one facet, from the geometrical three-dimensional configuration of crack growth, without regard to triple points acting as barriers.

The present results for 304 stainless steel do not support the model of step-wise crack growth because of the presence of a non-negligible number of cracks which have lengths $\frac{1}{3} < l < 1$. However, the result that the majority of the cracks occur for the tensile specimens where $l = 1$ and for the creep-rupture specimens where $l = 1$ and $0 < l \leqq \frac{1}{3}$ is interpreted to mean that, once formed, a crack has a higher probability of traversing an entire facet than of stopping at some intermediate point.

This result, combined with the observation that few cracks were found to have lengths greater than one facet, indicates that the grain-boundary triple points do constitute a significant barrier to crack propagation in this material, in addition to providing preferred crack nucleation sites.

A recent analysis of cavity growth by grain-boundary sliding [13], has predicted that the growth rate, in terms of cavity length change as a function of sliding displacement, depends on both cavity length and the angle between the direction of applied stress and the cavitated grain boundary. From this prediction, the cavities which grow at the fastest rate occur at the largest angle and have the longest length.

The present results for type 304 stainless steel show that the angular orientation of a crack with respect to the applied stress depends more on the deformation rate during testing than on crack length. This is because the angle at which the maximum fraction of cracks occurs remains relatively constant for a given deformation rate irrespective of crack length (see Fig. 2). With a decreasing deformation rate, this angle increases to a value near 80°, again irrespective of crack length.

These results are not unexpected because it is generally observed that grain-boundary sliding is related to the degree of deformation directly with the test temperature and inversely with the applied stress. It is the grain-boundary sliding which primarily contributes to grain rotation to a more favourable angular orientation for intergranular crack formation and growth. Therefore, since the deformation rate is directly related to the applied stress, the angular orientation of the maximum fraction of cracks in specimens tested at a common temperature is expected to be inversely controlled by the deformation rate.

It was also observed that the maximum crack width (or wedge height) generally increases with increasing angular orientation and increasing crack length for the creep-rupture specimens. This is illustrated in Fig. 4 using the same crack length intervals previously employed in Figs. 1 and 2. A similar observation was made for the tensile specimens but quantitative data were not obtained. Theory shows that the length of a wedge crack is a function of the crack width [12], which is, in turn, a function of the grain-boundary sliding rate [18].

These results suggest that the crack growth rate, which is taken to represent the change in crack volume as a function of time for the present case, will be more dependent on the angular orientation of the cracks and crack width than on crack length. If we now assume that this crack growth rate is directly related to only the angle at which the maximum fraction of

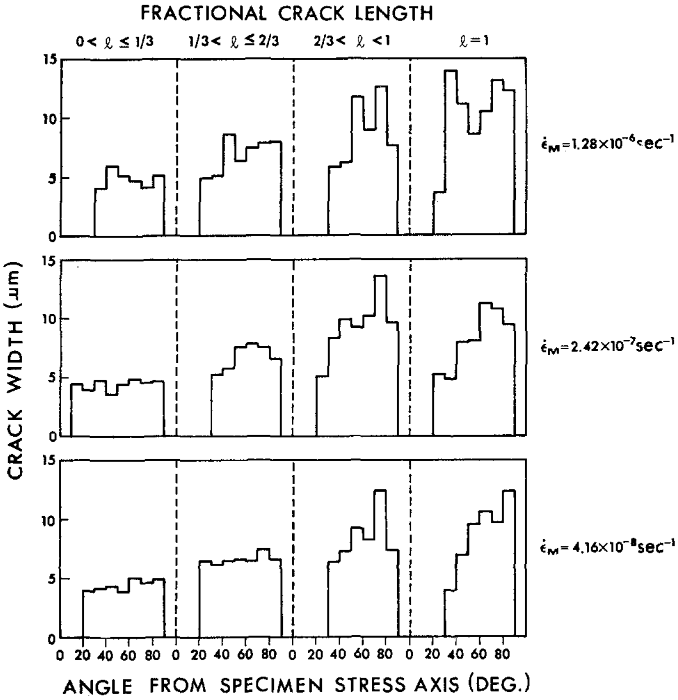

Figure 4 Crack width as a function of angle for the creep-rupture specimens.

cracks is observed, it is evident that the crack growth rate must have remained constant at a given deformation rate. This implies that the crack growth rate will increase with decreasing deformation rate and increasing crack angle, independent of crack length, in agreement with the experimental observations.

Thus, the angular orientation of a cracked grain boundary and the associated crack width, as a function of the deformation rate, are concluded to be the most important parameters which reflect the growth rate of cracks in 304 stainless steel under the test conditions employed in this work. Furthermore, this conclusion suggests that the change of crack volume as a function of test time, rather than measurements of individual crack width, angle, and length parameters, may more closely approximate the actual crack growth behaviour of this material. Data concerning this point are presently being obtained by the authors.

Acknowledgements

This investigation was supported by the US Atomic Energy Commission under Contract AT(11-1)-2107. The authors are pleased to acknowledge the assistance of R. W. Swindeman, Oak Ridge National Laboratory, who kindly provided the tested specimens, their fabrication details, and the test results.

References

1. U. LINDBORG, *Acta Metallurgica* **17** (1969) 157.
2. U. LINDBÖRG and B. O. GUSTAFSSON, "Fracture 1969", Ed. P. L. Pratt, (Chapman and Hall, London, 1969), p. 457.
3. R. SÖDERBERG, *ibid*, p. 450.
4. J. S. WADDINGTON and K. LOFTHOUSE, *J. Nucl. Mat.* **22** (1967) 205.
5. A. GITTINS, *J. Mater. Sci.* **5** (1970) 223.
6. H. C. CHANG and N. J. GRANT, *Trans. AIME* **206** (1956) 544.
7. D. M. R. TAPLIN, *J. Aust. Inst. Met.* **10** (1965) 336.
8. C. ZENER, "Elasticity and Anelasticity of Metals", (University of Chicago Press, Chicago, 1948), p. 158.
9. A. N. STROH, *Proc. Roy. Soc.* **A223** (1954) 404; *Adv. Phys.* **6** (1957) 418.
10. A. H. COTTRELL, *Trans. AIME* **212** (1958) 192.
11. R. BULLOUGH, *Phil. Mag.* **9** (1964) 917.
12. J. A. WILLIAMS, *ibid*, **15** (1967) 1289.
13. H. E. EVANS, *ibid*, **23** (1971) 1101.
14. D. J. MICHEL, H. NAHM, and J. MOTEFF, to be published in *Mat. Sci. Eng.* (1972).
15. P. W. DAVIES, K. R. WILLIAMS, and B. WILSHIRE, *Phil. Mag.* **18** (1968) 197.
16. U. LINDBORG, *Scripta Met.* **3** (1969) 565.
17. R. C. GIFKINS, *ibid*, **3** (1969) 561.
18. P. T. HEALD and J. A. WILLIAMS, *Phil. Mag.* **24** (1971) 1215.

Received 27 May and accepted 13 August 1972.